

## Characterization of Zn-Substituted Nano-Sized $\text{CoAl}_2\text{O}_4$ Powder Synthesized by Egg-White Method

Y.M. AL-ANGARI<sup>1</sup>, M.A. GABAL<sup>1,†,\*</sup> and F.A. AL-AGEL<sup>2</sup>

<sup>1</sup>Chemistry Department, Faculty of Science, King Abdulaziz University, Jeddah, Kingdom of Saudi Arabia

<sup>2</sup>Physics Department, Faculty of Science, King Abdulaziz University, Jeddah, Kingdom of Saudi Arabia

†Permanent Address: Chemistry Department, Faculty of Science, Benha University, Benha, Egypt

\*Corresponding author: Tel: +966 557071572; E-mail: mgabalabdonada@yahoo.com

Received: 12 May 2014;

Accepted: 15 September 2014;

Published online: 1 December 2014;

AJC-16381

In the present study, a simple and environmental friendly egg-white was utilized for the preparation of nano-crystalline  $\text{Co}_{0.5}\text{Zn}_{0.5}\text{Al}_2\text{O}_4$ . The decomposition process of the precursor was followed through TG measurement. XRD, FT-IR and TEM techniques to characterize the produced aluminate. The obtained XRD pattern indicates the formation of single-phase cubic structure. FT-IR exhibited two characteristic bands of aluminate structure. TEM image showed cubic agglomerated particles with an average size of about 20 nm. Ac-conductivity measurements indicates the semiconducting properties of the obtained aluminate with room temperature conductivity of  $3.4 \times 10^{-4} \Omega^{-1} \text{cm}^{-1}$ .

**Keywords:** Co-Zn $\text{Al}_2\text{O}_4$ , Egg-white method, Ac-conductivity, XRD, FT-IR.

### INTRODUCTION

Thernard's blue;  $\text{CoAl}_2\text{O}_4$  spinel is one of the most popular inorganic pigments<sup>1</sup>. Its physicochemical features, such as high thermal and chemical stability, high resistance to acids, alkalis, light and various atmospheric agents make it suitable for various industrial applications, such as ceramics, glass, plastics, paint, paper, rubber and color TV tubes<sup>2-4</sup>.

$\text{CoAl}_2\text{O}_4$  has been conventionally synthesized using solid-state method<sup>5</sup> at temperatures above 1000 °C, for long periods of time. Wet-chemical methods have also been extensively applied, among them: coprecipitation method<sup>6</sup>, hydrothermal synthesis<sup>7</sup>, sol-gel route<sup>8</sup>, low temperature combustion synthesis<sup>9</sup>, complexation method<sup>10</sup>.

The key elements for  $\text{CoAl}_2\text{O}_4$  is the constituent of cobalt, which is the source of the observed blue color<sup>1,11</sup>. However, the preparation of blue aluminate pigments suffers several disadvantages that arise from the fact that cobalt is scarce, expensive and, most importantly, toxic. In this context, the reduction of the cobalt content of such oxide pigments would prove of value, from an environmental perspective, assuming that its coloration properties could be maintained.

Many researchers studied CoZnAl system. Visinescu *et al.*<sup>1</sup> prepared nano-sized  $\text{Co}_x\text{Zn}_{1-x}\text{Al}_2\text{O}_4$  ( $x = 0.0-1.0$ ) using a novel, starch-based synthetic route. The system was characterized using fourier transform infrared (FT-IR), X-ray diffraction (XRD) and scanning electron microscopy (SEM).

de Souza *et al.*<sup>8</sup> synthesized  $\text{Co}_x\text{Zn}_{1-x}\text{Al}_2\text{O}_4$  system ( $x = 0.0-1.0$ ) by polymeric precursor method. X-ray diffraction, differential thermal analysis-thermogravimetry (DTA-TG), IR, ultraviolet-visible spectroscopy and colorimetry techniques are used to characterize the system.

Barroso *et al.*<sup>11</sup> prepared CoZnAl catalysts through citrate sol-gel method and characterized by different techniques such as atomic absorption, TG, BET, TPR, XRD, Raman and SEM-EDX techniques.

In this study we will report an environmental friendly synthesis method for this oxide-based pigments. A novel, less-toxic, flexible, economic and reproducible egg-white method<sup>12-15</sup> will be used for the synthesis of zinc-substituted cobalt aluminate oxide spinels;  $\text{Co}_{0.5}\text{Zn}_{0.5}\text{Al}_2\text{O}_4$ . In this method, the egg-white has a triple role during the synthesis as complexing, template and gelation agent. The thermal decomposition of the as-prepared precursor will be followed by TG technique up to aluminate formation. The prepared aluminates will be characterized using XRD, FT-IR and TEM. In addition, the electrical properties as a function of temperature and frequency will be measured.

### EXPERIMENTAL

The starting materials;  $\text{Co}(\text{NO}_3)_2 \cdot 6\text{H}_2\text{O}$ ,  $\text{Zn}(\text{NO}_3)_2 \cdot 6\text{H}_2\text{O}$ ,  $\text{Al}(\text{NO}_3)_3 \cdot 9\text{H}_2\text{O}$  are all of analytical reagent and were used as supplied. Stoichiometric amounts of nitrates to assure the composition to reach  $\text{Co}_{0.5}\text{Zn}_{0.5}\text{Al}_2\text{O}_4$  were mixed with 60 mL of

freshly extracted egg-white as in the procedure previously described<sup>13,15</sup>. The resultant gel were evaporated until dryness and the obtained as-prepared precursor was then calcined in an electric oven at 800 °C for 2 h.

**Techniques:** The thermal decomposition behavior of the as-prepared egg-white precursor was followed through thermogravimetry technique (TG) using a Perkin-Elmer, STA 6000 thermal analyzer up to 800 °C at a heating rate of 5 °C/min in air atmosphere.

The aluminates formation, phase purity and crystallinity were identified by X-Ray diffraction technique using a Bruker D8 high-resolution diffractometer with nickel filtered  $\text{Cu-K}\alpha 1$  radiation. Lattice parameter, cell volume, X-Ray density and the crystallite size were calculated using equations from<sup>15</sup>.

Fourier transform infrared (FT-IR) spectra were recorded in the range 1000-200  $\text{cm}^{-1}$  on JASCO FT-IR 310 spectrometer using KBr pellet method. TEM images of the obtained aluminate was monitored using a JEOL 2010 transmission electron microscopy operated at 80 kV. The electrical measurements, were carried out on a pressed pellets (1 cm in diameter and about 1 mm in thickness) coated with silver paste, in the frequency range 100 Hz-5 MHz up to 550 K, using a Hioki LCR bridge model 3531.

## RESULTS AND DISCUSSION

**Thermal decomposition of the gel-precursor and aluminate formation:** Fig. 1 shows TG-DTG curves of the gel-precursor with  $x = 0.5$ . From the figure, it is obvious that the decomposition proceeds through four overlapped steps up to about 550 °C after which a constant weight loss was obtained. According to the decomposition temperature range, the first two steps can be attributed to the dehydration of the precursor. The following steps represent the combustion reaction between the organic moiety (egg-white) as a fuel and nitrates act as an oxidant. No further weight losses can be obtained even by rising the temperature up to 800 °C.

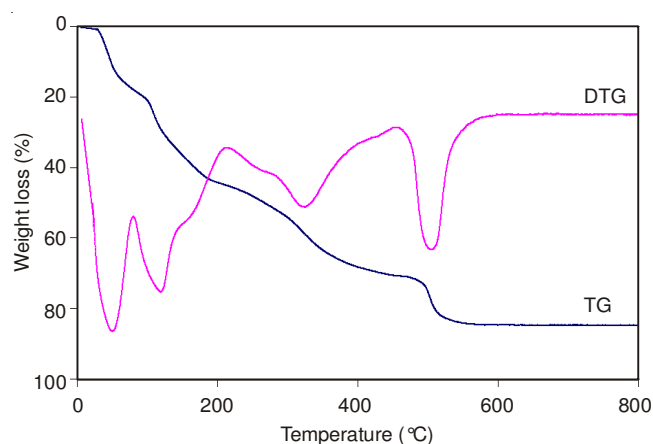


Fig. 1. DTA-TG curves in air of gel-precursor with  $x = 0.5$ . Heating rate = 5 °C  $\text{min}^{-1}$

**X-Ray diffraction study:** X-Ray diffraction of the as-prepared powder produced an amorphous material with few weak broad peaks between  $2\theta$  values of 30° and 40° which could not be identified as crystalline phases of zinc or cobalt aluminates. Fig. 2 shows X-Ray diffraction patterns of the

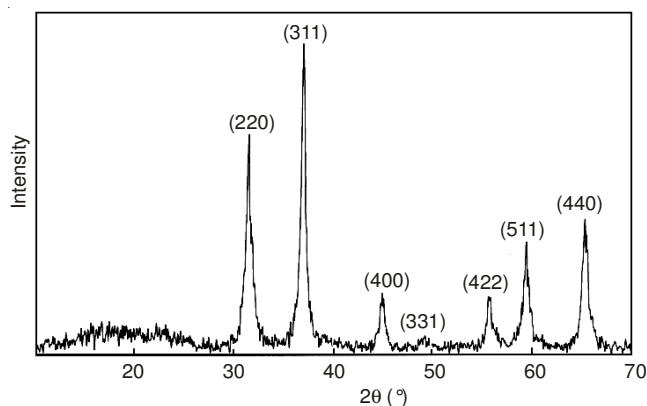


Fig. 2. XRD pattern of the precursor calcined at 800 °C

calcined powders at 800 °C. All the observed peaks are attributed to a single-phase cubic polycrystalline  $\text{CoZnAl}_2\text{O}_4$  (JCPDF file No. 76-0070) without any indication for the presence of secondary phases which suggests the complete formation of aluminate phase.

The considerable broadening of the diffraction peaks indicates nano-sized characteristics of the calcined powder. The crystallite size calculated from the half-width of the diffraction peaks using Scherrer's formula<sup>15</sup> amounts to 19 nm. In addition the calculated lattice parameter ( $a$ ) and X-Ray density ( $D_x$ )<sup>16</sup> are 8.071 Å and 4.55  $\text{g cm}^{-3}$ , respectively.

**FT-IR spectrum:** Fig. 3 shows FT-IR spectrum of the calcined powder at 800 °C. From the Figure, it should be noticed that, two stretching vibration bands in the range 500-800  $\text{cm}^{-1}$  are appeared. It is well known that, spinels structure display two stretching bands in the range 500-900  $\text{cm}^{-1}$ , associated with the vibrations of metal-oxygen, aluminum-oxygen and metal-oxygen-aluminum<sup>17-19</sup>. These two stretching bands can be ascribed, in accordance to the literature data<sup>20,21</sup>, to cobalt zinc aluminate spinel.

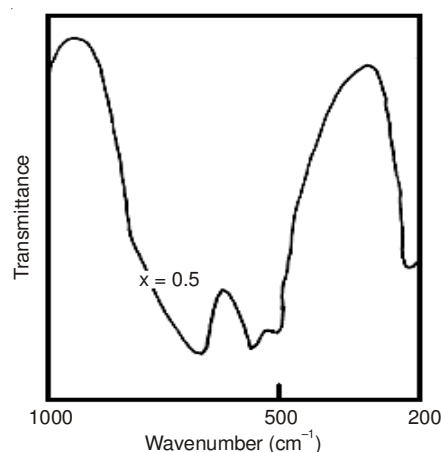


Fig. 3. FT-IR spectrum of  $\text{Co}_{0.5}\text{Zn}_{0.5}\text{Al}_2\text{O}_4$

**Transmission electron microscopy:** Transmission electron microscopy image of the prepared aluminate sample (Fig. 4) exhibited regularly shaped agglomerated cubic particles with average size of about 20 nm agrees well with that estimated through XRD measurement. The agglomeration characteristic can be attributed to electrostatic or van der Waals forces created between particles<sup>22</sup>.

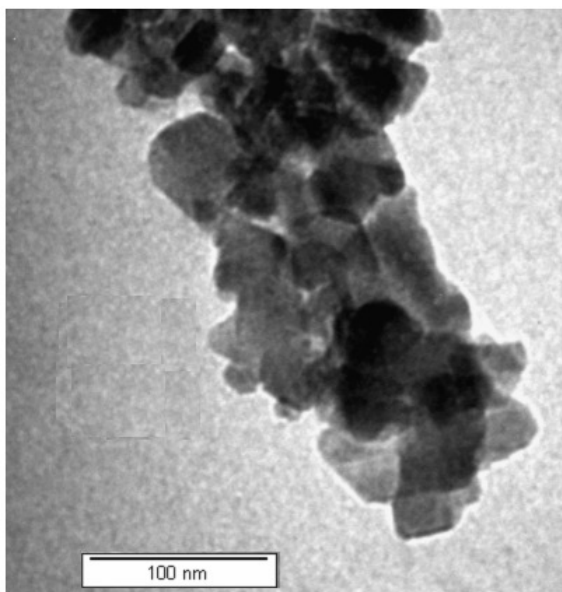


Fig. 4. TEM image of  $\text{Co}_{0.5}\text{Zn}_{0.5}\text{Al}_2\text{O}_4$ ; (scale bar: 100 nm)

**Ac-conductivity measurement:** The measured Ac-conductivity as a function of temperature and frequency for  $\text{Co}_{0.5}\text{Zn}_{0.5}\text{Al}_2\text{O}_4$  is illustrated in Fig. 5. The observed metallic behavior predominated at low temperatures region up to about 450 K, in which the conductivity decreases with increasing temperature, can be ascribed to the evaporation of adsorbed water molecules, which usually behave as an electron donor<sup>23</sup>. At higher temperatures, the plot of  $\ln \sigma$  vs.  $1/T$  obeys the Arrhenius relation, indicating the semiconducting behavior of the entire aluminate. The room temperature conductivity value (calculated at 10 kHz) is  $3.4 \times 10^{-4} \Omega^{-1} \text{cm}^{-1}$ . The calculated activation energy in this region amounts to about 1.9 eV.

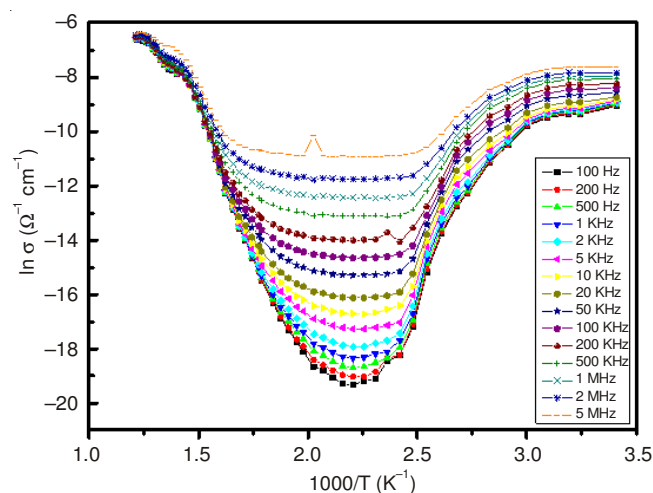


Fig. 5. Relation between  $\ln \sigma$  and reciprocal of absolute temperature as a function of applied frequency for  $\text{Co}_{0.5}\text{Zn}_{0.5}\text{Al}_2\text{O}_4$

The increase in conductivity with increasing frequency can be attributed to the pumping force transferring charge carriers between different localized states as well as liberating trapped charges from different trapping centers<sup>24</sup>.

## Conclusion

Nano-sized  $\text{Co}_{0.5}\text{Zn}_{0.5}\text{Al}_2\text{O}_4$  was successfully synthesized through simple, economic and environmentally friendly egg-white method. XRD indicates the formation of single phase cubic spinel structure. FT-IR measurement exhibited the characteristic vibration bands of the spinel. TEM image showed average crystallite size of about 20 nm agrees well with that estimated through XRD measurements. Ac-conductivity measurements indicate the semiconducting behaviour of the obtained aluminate.

## ACKNOWLEDGEMENTS

This project was funded by the Deanship of Scientific Research (DSR), King Abdulaziz University, Jeddah, under grant No. [76-130-1433]. The authors therefore, Acknowledge with thanks DSR technical and financial support.

## REFERENCES

1. D. Visinescu, C. Paraschiv, A. Ianculescu, B. Jurca, B. Vasile and O. Carp, *Dyes Pigments*, **87**, 125 (2010).
2. W. Li, J. Li and J. Guo, *J. Eur. Ceram. Soc.*, **23**, 2289 (2003).
3. P. Thormählen, E. Fridell, N. Cruise, M. Skoglundh and A. Palmqvist, *Appl. Catal. B*, **31**, 1 (2001).
4. D.M.A. Melo, J.D. Cunha, J.D.G. Fernandes, M.I. Bernardi, M.A.F. Melo and A.E. Martinelli, *Mater. Res. Bull.*, **38**, 1559 (2003).
5. T. Suzuki, H. Nagai, M. Nohara and H. Takagi, *J. Phys. Condens. Matter*, **19**, 145265 (2007).
6. D. Rangappa, S. Ohara, T. Naka, A. Kondo, M. Ishii and T. Adschiri, *J. Mater. Chem.*, **17**, 4426 (2007).
7. Z.Z. Chen, E.W. Shi, Y.Q. Zheng, B. Xiao and J.Y. Zhuang, *J. Am. Ceram. Soc.*, **86**, 1058 (2003).
8. L. Desouza, J. Zamian, G. Darochafilho, L. Soledade, I. Dossantos, A. Souza, T. Scheller, R. Angelica and C. Dacosta, *Dyes Pigments*, **81**, 187 (2009).
9. C. Suci, I. Mindru, G. Marinescu, L. Patron, O. Carp and V.S. Teodorescu, *J. Optoelectron. Adv. Mater.*, **10**, 2703 (2008).
10. C. Wang, S. Liu, L. Liu and X. Bai, *Mater. Chem. Phys.*, **96**, 361 (2006).
11. R.K. Mason, *Bull. Am. Ceram. Soc.*, **40**, 5 (1961).
12. M.N. Barroso, M.F. Gomez, L.A. Arrúa and M.C. Abello, *Chem. Eng. J.*, **158**, 225 (2010).
13. M.A. Gabal, *Mater. Lett.*, **64**, 1887 (2010).
14. M.A. Gabal, A.M. Asiri and Y.M. Al Angari, *Ceram. Int.*, **37**, 2625 (2011).
15. M.A. Gabal, R.M. El-Shishtawy and Y.M. Al Angari, *J. Magn. Magn. Mater.*, **324**, 2258 (2012).
16. B. Ismail, S.T. Hussain and S. Akram, *Chem. Eng. J.*, **219**, 395 (2013).
17. D. Dhak and P. Pramanik, *J. Am. Ceram. Soc.*, **89**, 1014 (2006).
18. K. Nakamoto, *Infrared Spectra of Inorganic and Coordination Compound*, Chemical Industry Press, Beijing, edn 4 (1991).
19. L.K.C. de Souza, J.R. Zamian, G.N. da Rocha Filho, L.E.B. Soledade, I.M.G. dos Santos, A.G. Souza, T. Scheller, R.S. Angélica and C.E.F. da Costa, *Dyes Pigments*, **81**, 187 (2009).
20. M. Zawadzki, W. Staszak, F.E. Lopez-Suarez, M.J. Illan-Gomez and A. Bueno-Lopez, *App. Catal. A*, **371**, 92 (2009).
21. Z. Chen, E. Shi, W. Li, Y. Zheng and W. Zhong, *Mater. Lett.*, **55**, 281 (2002).
22. M.A. Gabal, *J. Magn. Magn. Mater.*, **321**, 3144 (2009).
23. A.K. Nikumbh, R.A. Pawar, D.V. Nighot, G.S. Gugale, M.D. Sangale, M.B. Khanvilkar and A.V. Nagawade, *J. Magn. Magn. Mater.*, **355**, 201 (2014).
24. M.A. Dar, K.M. Batoo, V. Verma, W.A. Siddiqui and R.K. Kotnala, *J. Alloys Comp.*, **493**, 553 (2010).